

Weighted MMSE Precoding for Constructive Interference Region

Yafei Wang, *Student Member, IEEE*, Wenjin Wang, *Member, IEEE*, Li You, *Senior Member, IEEE*, Christos G. Tsinos, *Senior Member, IEEE*, Shi Jin, *Senior Member, IEEE*

arXiv:2210.00167v1 [cs.IT] 1 Oct 2022

Abstract—In this paper, we propose a symbol-level precoding (SLP) design that aims to minimize the weighted mean square error between the received signal and the constellation point located in the constructive interference region (CIR). Unlike most existing SLP schemes that rely on channel state information (CSI) only, the proposed scheme exploits both CSI and the distribution information of the noise to achieve improved performance. We firstly propose a simple generic description of CIR that facilitates the subsequent SLP design. Such an objective can further be formulated as a nonnegative least squares (NNLS) problem, which can be solved efficiently by the active-set algorithm. Furthermore, the weighted minimum mean square error (WMMSE) precoding and the existing SLP can be easily verified as special cases of the proposed scheme. Finally, simulation results show that the proposed precoding outperforms the state-of-the-art SLP schemes in full signal-to-noise ratio ranges in both uncoded and coded systems without additional complexity over conventional SLP.

Index Terms—WMMSE, symbol-level precoding, constructive interference region, low complexity.

I. INTRODUCTION

IN multiuser multi-input multi-output (MU-MIMO) downlink transmission, precoding is employed to suppress user interference and to obtain spatial multiplexing and array gain. Linear precoding, e.g., zero-force (ZF) and weighted minimum mean square error (WMMSE) [1], [2], constructs the precoding matrix based on channel state information. Although linear precoding is widely adopted due to its low complexity, it cannot approach theoretical system capacity. In contrast, nonlinear precoding further improves the performance by designing the precoding scheme with input data, e.g., dirty paper coding (DPC) [3], vector perturbation (VP) precoding [4], and symbol-level-precoding (SLP) [5]–[12].

Among wireless nonlinear precoding, SLP exploits interference with the transmitted data symbols and their corresponding constellations to design precoding schemes symbol-by-symbol [5]–[12]. The concept of constructive interference (CI) and destructive (DI) was proposed in [13], based on which the CI region (CIR) was defined, and precoding was therefore specifically optimized for phase-shift keying (PSK) in [7], [14]. The definition of CIR in PSK was further extended to quadrature amplitude modulation (QAM) [9], [11], [12], where the inner constellations were fixed, and outer constellations could be expanded. Furthermore, SLP is proved to be the generalization of ZF precoding in [10] and [6], and it is also represented by the form of symbol-perturbed ZF precoding in [15] and [16].

Although the existing SLP solutions achieve significant performance gains over ZF precoding in the high SNR regime

by exploiting CI, they are inferior to WMMSE precoding in the low signal-to-noise ratio (SNR) regime as they only control interference but ignore the impact of the noise, while WMMSE utilizes distribution information of the noise [8], [17], [18]. This raises a key question: *How to exploit both CI and the distribution information of the noise to optimize precoding design in full SNR ranges?* In this paper, we try to provide an answer. Firstly, we propose a simple generic description of CIR, which can facilitate the related SLP designs. Then, we develop CI-WMMSE precoding for the first time, which minimizes the weighted mean square error between the received signal and the target signal in CIR. CI-WMMSE is expected to perform better since it synthetically utilizes the noise distribution and CIR. There is a remarkable conclusion that the WMMSE and the existing SLP can be verified as special cases of CI-WMMSE. Based on our CIR description, CI-WMMSE is formulated as a nonnegative least squares (NNLS) problem, which can be efficiently solved [19]. Finally, simulation results show the superiority of CI-WMMSE in full SNR ranges in both coded and uncoded systems.

II. SYSTEM MODEL

Consider a downlink system where a N -antenna base station (BS) transmits information to K single-antenna user equipments (UE). The channel between the BS and the k -th UE is denoted as $\mathbf{h}_k \in \mathbb{C}^{N \times 1}$. The channel matrix $\mathbf{H} = [\mathbf{h}_1, \mathbf{h}_2, \dots, \mathbf{h}_K]^T$ is assumed to be available at the BS. At a symbol duration, K independent QAM or PSK symbols are intended to be transmitted to K UEs, and the symbols are denoted as $\mathbf{s} = [s_1, s_2, \dots, s_K]^T \in \mathbb{C}^{K \times 1}$, where s_k is the symbol to be transmitted to the k -th UE. The symbol vector \mathbf{s} is mapped to the transmit vector $\mathbf{u} \in \mathbb{C}^{N \times 1}$ by applying the symbol-level precoder represented by SLP (\cdot), which can be expressed as

$$\mathbf{u} = \text{SLP}(\mathbf{s}, \mathbf{H}, \sigma^2), \quad (1)$$

where σ^2 denotes the variance of the additive noise n_k following zero-mean complex Gaussian distribution at the k -th UE. The received signal at the k -th UE is given by

$$y_k = \mathbf{h}_k^T \mathbf{u} + n_k, \quad \forall k \in \mathcal{K}, \quad (2)$$

where $\mathcal{K} = \{1, 2, \dots, K\}$. When multi-level modulations (e.g., 16QAM and 64QAM) are employed, the received signals require to be scaled for correct demodulation, i.e.,

$$\hat{y}_k = \frac{a_k}{\gamma} (\mathbf{h}_k^T \mathbf{u} + n_k), \quad (3)$$

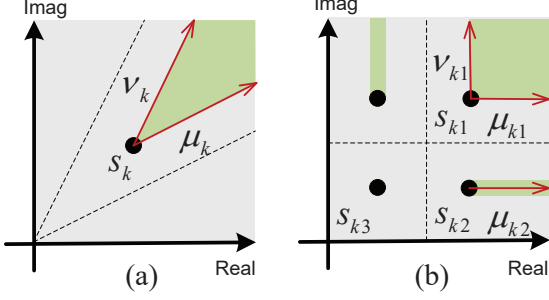


Fig. 1. CIRs and their boundary vectors of (a) PSK and (b) QAM.

where $a_k \in \mathbb{C}$ is a nonzero complex that denotes the pre-determined processing coefficient at k -th UE, and $\gamma \in \mathbb{R}$ is a gain factor in the precoding scheme which scales the signal to satisfy the symbol-level transmit power constraint $\|\mathbf{u}\|_2^2 \leq P_T$, where P_T is the transmit power budget. By omitting the noise component of \hat{y}_k , $(a_k/\gamma)\mathbf{h}_k^T \mathbf{u}$ is termed as the noise-free received signal.

III. WMMSE CRITERION FOR CONSTRUCTIVE INTERFERENCE REGION

In conventional SLP transmission, CI is defined as the interference that pushes the noise-free received signal further away from the decision boundaries. CI region (CIR) is the modulation-specific region where the interference component of the received signal is CI [5], [6], [11]. In this Section, we firstly propose a simple parameterized description of CIR, which can facilitate subsequent SLP design.

A. A Simple Generic Description of CIR

The CIR for PSK and QAM constellations, whose geometric definitions have been well investigated [6], are shown in the green areas of Fig. 1, where the dotted lines represent the decision boundaries based on the maximum likelihood (ML) decision rule [11]. The CIRs, composed of two or fewer boundaries (including those of PSK and QAM), can be described by the transmitted symbol and its CIR boundary parameters. Specifically, the CIR belongs to s_k in Fig. 1 can be expressed as

$$\mathcal{D}_k = \{\tilde{s}_k \mid \tilde{s}_k = s_k + \delta_{\mu_k} \mu_k + \delta_{\nu_k} \nu_k, \delta_{\mu_k}, \delta_{\nu_k} > 0\}, \quad (4)$$

where μ_k and ν_k are two normal boundary parameters of the CIR belonging to s_k , which can be easily obtained from s_k . We define the following diagonal matrixes

$$\begin{aligned} \mathbf{M}_R &= \text{diag}\{\Re(\mu_1), \dots, \Re(\mu_K)\}, \\ \mathbf{M}_I &= \text{diag}\{\Im(\mu_1), \dots, \Im(\mu_K)\}, \\ \mathbf{N}_R &= \text{diag}\{\Re(\nu_1), \dots, \Re(\nu_K)\}, \\ \mathbf{N}_I &= \text{diag}\{\Im(\nu_1), \dots, \Im(\nu_K)\}, \end{aligned} \quad (5)$$

and construct a block diagonal matrix $\boldsymbol{\Lambda} = \begin{bmatrix} \mathbf{M}_R & \mathbf{N}_R \\ \mathbf{M}_I & \mathbf{N}_I \end{bmatrix}$. Since real and imaginary parts of $\tilde{s}_k \in \mathcal{D}_k$ can be expressed as

$$\begin{aligned} \Re(\tilde{s}_k) &= \Re(s_k) + \delta_{\mu_k} \Re(\mu_k) + \delta_{\nu_k} \Re(\nu_k), \\ \Im(\tilde{s}_k) &= \Im(s_k) + \delta_{\mu_k} \Im(\mu_k) + \delta_{\nu_k} \Im(\nu_k), \end{aligned} \quad (6)$$

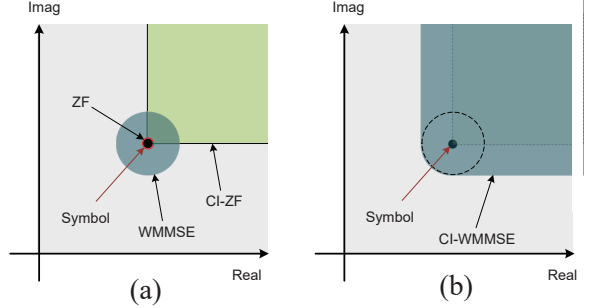


Fig. 2. Distribution area of noise-free received signal for (a) conventional precoding schemes and (b) CI-WMMSE (our SLP scheme).

we further define $\boldsymbol{\delta} = [\delta_{\mu_1}, \dots, \delta_{\mu_K}, \delta_{\nu_1}, \dots, \delta_{\nu_K}]^T$, based on which the real and imaginary parts of signal vector $\tilde{\mathbf{s}} = [\tilde{s}_1, \tilde{s}_2, \dots, \tilde{s}_K]^T$ with the constraint

$$s.t. \tilde{s}_k \in \mathcal{D}_k, \forall k \in \mathcal{K}, \quad (7)$$

can be equivalently expressed as

$$\begin{bmatrix} \Re(\tilde{\mathbf{s}}) \\ \Im(\tilde{\mathbf{s}}) \end{bmatrix} = \begin{bmatrix} \Re(\mathbf{s}) \\ \Im(\mathbf{s}) \end{bmatrix} + \boldsymbol{\Lambda} \boldsymbol{\delta}, \boldsymbol{\delta} \succeq 0. \quad (8)$$

Notice that such a simple and clear generic description can significantly facilitate the following derivations.

B. Constructive-Interference WMMSE Precoding

As shown in the red area in Fig. 2(a), ZF precoding restrains the noise-free received signal at the position of transmitted symbol s_k , aiming to suppress all interference. Over the low SNR regime, since ZF precoding ignores the impact of noise, it underperformed WMMSE precoding [6]. Given the noise distribution, WMMSE allowed the noise-free received signal to be distributed around s_k as the dark area in Fig. 2(a) to minimize the weighted mean square error (MSE) between \hat{y}_k and s_k . As the green area in Fig. 2(a) shows, CI-ZF precoding (i.e., the conventional SLP [6], [7], [10], [16], [20]) allows the noise-free received signal to distribute in the CIR, which relaxes the constraints on interference. Similar to ZF, CI-ZF also ignores the impact of the noise and thus can only achieve performance gain in high SNR regimes. One potential way to improve precoding performance is to exploit both the benefit of CIR and the noise distribution. To this end, we investigate the CI-WMMSE precoding, aiming to minimize the weighted MSE between \hat{y}_k and the expected received signal \hat{s}_k located in CIR \mathcal{D}_k . Define $\mathbf{u} = \gamma \mathbf{x}$, where $\gamma = \sqrt{\frac{P_T}{\|\mathbf{x}\|_2^2}}$ is the symbol-level power scaling factor, and \mathbf{x} is the transmit signal without power constraint. Then (3) can be rewritten as

$$\hat{y}_k = a_k \mathbf{h}_k \mathbf{x} + \frac{a_k n_k}{\gamma}. \quad (9)$$

Thus, the problem of CI-WMMSE can be expressed as

$$\begin{aligned} \min_{\mathbf{x}, \tilde{\mathbf{s}}} \mathbb{E}_{\mathbf{n}} &\left\{ \left\| \boldsymbol{\Omega}^{\frac{1}{2}} \left[\mathbf{A} \left(\mathbf{H} \mathbf{x} + \frac{\mathbf{n}}{\gamma} \right) - \tilde{\mathbf{s}} \right] \right\|_2^2 \right\} \\ s.t. \tilde{s}_k &\in \mathcal{D}_k, \forall k \in \mathcal{K}, \end{aligned} \quad (10)$$

where $\mathbf{A} = \text{diag}\{a_1, a_2, \dots, a_K\}$, $\Omega = \text{diag}\{\omega_1, \omega_2, \dots, \omega_K\}$, $\tilde{\mathbf{s}}$ denotes the vector of signals located in CIR defined in (7) and (8), ω_k represents the weight belonging to the MSE of k -th UE, and $\mathbb{E}_{\mathbf{n}} \{\cdot\}$ denotes taking an expectation over \mathbf{n} . As Fig. 2(b) shows, CI-WMMSE relaxes the constraint in WMMSE that the expected received signal should be around the transmit symbol. By taking expectation over \mathbf{n} , (10) becomes

$$\begin{aligned} \min_{\mathbf{x}, \tilde{\mathbf{s}}} & \left\| \Omega^{\frac{1}{2}} (\mathbf{A} \mathbf{H} \mathbf{x} - \tilde{\mathbf{s}}) \right\|_2^2 + \frac{\sigma^2 \text{Tr}(\Omega \mathbf{A} \mathbf{A}^H)}{P_T} \|\mathbf{x}\|_2^2 \\ \text{s.t. } & \tilde{s}_k \in \mathcal{D}_k, \forall k \in \mathcal{K}. \end{aligned} \quad (11)$$

Remark 1: The problems of WMMSE, MMSE, CI-ZF, and ZF precoding can be viewed as special cases of CI-WMMSE precoding.

1) WMMSE & MMSE: If we constrain $\tilde{\mathbf{s}} = \mathbf{s}$ and the precoding scheme as the linear precoding, i.e., $\mathbf{x} = \mathbf{W}\mathbf{s}$, the problem (10) degenerates into

$$\min_{\mathbf{W}} \mathbb{E}_{\mathbf{n}} \left\{ \left\| \Omega^{\frac{1}{2}} \left[\mathbf{A} \left(\mathbf{H} \mathbf{W} \mathbf{s} + \frac{\mathbf{n}}{\gamma} \right) - \mathbf{s} \right] \right\|_2^2 \right\}. \quad (12)$$

The above problem is equivalent to the conventional WMMSE except for the definition of γ . Unlike power scaling factor $\gamma = \sqrt{\frac{P_T}{\|\mathbf{W}\mathbf{s}\|_2^2}}$ defined in (12), conventional WMMSE defines it as $\gamma = \frac{P_T}{\text{Tr}(\mathbf{W}\mathbf{W}^H)}$ [17], which means the former is constrained by symbol-level power and the latter by average power. Consequently, as a special case of CI-WMMSE, problem (12) can be seen as symbol-level power constrained WMMSE. When the power allocation scheme in [8] is employed and the number of symbol groups involving in the scheme approaches infinity, problem (12) with symbol-level power constraint can be easily verified to be equivalent to that with average power constraint, since the average power constraint can be regarded as a power allocation scheme between symbols. When $\Omega = \mathbf{I}_K$, problem (12) will further degenerate into MMSE [21].

2) CI-ZF & ZF: When $\Omega = \mathbf{I}_K$ and $\sigma \rightarrow 0$, the left part of the cost function in (11) can be seen as a constraint $\|\mathbf{A} \mathbf{H} \mathbf{x} - \tilde{\mathbf{s}}\|_2^2 = 0$, and the right part $\|\mathbf{x}\|_2^2$ becomes the primary cost function, based on which CI-WMMSE (11) is transformed into

$$\begin{aligned} \min_{\mathbf{x}} & \|\mathbf{x}\|_2^2 \\ \text{s.t. } & \mathbf{h}_k^T \mathbf{x} \in a_k^{-1} \mathcal{D}_k, \forall k \in \mathcal{K}, \end{aligned} \quad (13)$$

which can be easily verified to be equivalent to the problem of CI-ZF in [12]. Furthermore, if we set $\mathbf{A} = \mathbf{I}_K$ and $\tilde{\mathbf{s}} = \mathbf{s}$, \mathbf{x} is only subjected to the constraint $\|\mathbf{H} \mathbf{x} - \mathbf{s}\|_2^2 = 0$ which is the problem of ZF.

Considering the equivalent expression of $\tilde{\mathbf{s}}$ in (8), the representation of (11) in the real numbers' domain can be written as

$$\min_{\bar{\mathbf{x}}, \delta \geq 0} \left\| \Omega^{\frac{1}{2}} (\bar{\mathbf{A}} \bar{\mathbf{H}} \bar{\mathbf{x}} - (\bar{\mathbf{s}} + \Lambda \delta)) \right\|_2^2 + \frac{\sigma^2 \text{Tr}(\bar{\Omega} \bar{\mathbf{A}} \bar{\mathbf{A}}^T)}{P_T} \|\bar{\mathbf{x}}\|_2^2, \quad (14)$$

where

$$\begin{aligned} \bar{\mathbf{s}} &= \begin{bmatrix} \Re(\mathbf{s}) \\ \Im(\mathbf{s}) \end{bmatrix}, \bar{\Omega} = \begin{bmatrix} \Omega & \\ & \Omega \end{bmatrix}, \bar{\mathbf{x}} = \begin{bmatrix} \Re(\mathbf{x}) \\ \Im(\mathbf{x}) \end{bmatrix}, \\ \bar{\mathbf{A}} &= \begin{bmatrix} \Re(\mathbf{A}) & -\Im(\mathbf{A}) \\ \Im(\mathbf{A}) & \Re(\mathbf{A}) \end{bmatrix}, \bar{\mathbf{H}} = \begin{bmatrix} \Re(\mathbf{H}) & -\Im(\mathbf{H}) \\ \Im(\mathbf{H}) & \Re(\mathbf{H}) \end{bmatrix}. \end{aligned} \quad (15)$$

Define $\rho = \text{Tr}(\bar{\Omega} \bar{\mathbf{A}} \bar{\mathbf{A}}^T)$ and $\check{\mathbf{H}} = \bar{\mathbf{A}} \bar{\mathbf{H}}$, the gradient of $\bar{\mathbf{x}}$ is given by

$$\frac{\partial f}{\partial \bar{\mathbf{x}}} = 2\check{\mathbf{H}}^T \bar{\Omega} \check{\mathbf{H}} \bar{\mathbf{x}} - 2\check{\mathbf{H}}^T \bar{\Omega} (\bar{\mathbf{s}} + \Lambda \delta) + 2\frac{\sigma^2 \rho}{P_T} \bar{\mathbf{x}}, \quad (16)$$

where f denotes cost function in (14). Since f is a convex function over the open set of variables $\bar{\mathbf{x}}$, The optimal $\bar{\mathbf{x}}^*$ can be found by setting the gradient in (16) to zero and can be written as

$$\bar{\mathbf{x}}^* = \check{\mathbf{H}}^T \bar{\Omega} \left(\check{\mathbf{H}} \check{\mathbf{H}}^T \bar{\Omega} + \frac{\sigma^2 \rho}{P_T} \mathbf{I}_{2K} \right)^{-1} (\bar{\mathbf{s}} + \Lambda \delta). \quad (17)$$

By replacing $\bar{\mathbf{x}}$ in (14) with the formulation of $\bar{\mathbf{x}}^*$, (14) can be rewritten as (18).

$$\min_{\delta \geq 0} (\bar{\mathbf{s}} + \Lambda \delta)^T \left(\check{\mathbf{H}} \check{\mathbf{H}}^T + \frac{\sigma^2 \rho}{P_T} \bar{\Omega}^{-1} \right)^{-1} (\bar{\mathbf{s}} + \Lambda \delta). \quad (18)$$

As a quadratic programming problem with nonnegative constraints, the above formulation is further reformulated as a much simpler NNLS problem in the next subsection.

Remark 2: The optimal solutions of WMMSE, MMSE, CI-ZF, and ZF precoding can be viewed as special cases of CI-WMMSE precoding.

1) WMMSE & MMSE: When $\delta = 0$, the optimal solution (17) degenerates into real representations of WMMSE [17], which further degenerates into MMSE when $\bar{\Omega} = \mathbf{I}_{2K}$,

2) CI-ZF & ZF: When $\Omega = \mathbf{I}_K$ and $\sigma \rightarrow 0$, the optimal solution (17) degenerates into

$$\mathbf{x}_{CIZF}^* = \bar{\mathbf{H}}^T (\bar{\mathbf{H}} \bar{\mathbf{H}}^T)^{-1} (\bar{\mathbf{A}}^{-1} \bar{\mathbf{s}} + \bar{\mathbf{A}}^{-1} \Lambda \delta), \quad (19)$$

which can be easily verified as equivalent to CI-ZF in [20]. (19) will further degenerate into ZF when $\bar{\mathbf{A}} = \mathbf{I}_{2K}$ and $\delta = 0$.

C. Low-Complexity Algorithmic Solution

By obtaining the upper triangular matrix \mathbf{B} from the Cholesky decomposition $\mathbf{B}^T \mathbf{B} = \left(\check{\mathbf{H}} \check{\mathbf{H}}^T + \frac{\sigma^2 \rho}{P_T} \bar{\Omega}^{-1} \right)^{-1}$ and $\mathbf{d} = -\mathbf{B} \bar{\mathbf{s}}$, problem (18) can be written as

$$\min_{\delta \geq 0} \|\mathbf{B} \Lambda \delta - \mathbf{d}\|_2^2. \quad (20)$$

It can be observed that Λ is a diagonal matrix with some zero diagonal elements when \mathbf{s} includes QAM symbols. The zeros in the diagonal elements force the corresponding columns in $\mathbf{B} \Lambda$ and elements in δ to be zero during optimization. We denote \mathcal{T} and $K_{\mathcal{T}}$ as the index set of the non-zero diagonal elements of Λ and its cardinality, respectively. For different modulations, we have

$$\mathbb{E}_{\mathbf{s}} \{ K_{\mathcal{T}} \} = \begin{cases} K & \text{if } \mathbf{s} \text{ is modulated by 16QAM} \\ \frac{K}{2} & \text{if } \mathbf{s} \text{ is modulated by 64QAM} \\ 2K & \text{if } \mathbf{s} \text{ is modulated by PSK} \end{cases}. \quad (21)$$

We further define $\mathbf{B}_{[:,j \in \mathcal{T}]} / \Lambda_{[jj \in \mathcal{T}]} / \delta_{[j \in \mathcal{T}]}$ as the matrix/diagonal matrix/vector composed of the columns/diagonal elements/elements of $\mathbf{B}/\Lambda/\delta$ whose indices belong to set \mathcal{T} . Then, problem (20) is equivalent to

$$\min_{\delta_{[j \in \mathcal{T}]} \geq 0} \|\mathbf{B}_{[:,j \in \mathcal{T}]} \Lambda_{[jj \in \mathcal{T}]} \delta_{[j \in \mathcal{T}]} - \mathbf{d}\|_2^2. \quad (22)$$

Compared with (20), the dimension of δ is reduced from $2K$ to K_τ . Our low-complexity optimization (22) is also suitable for CI-ZF with NNLS-based solution since they have the similar matrix structure [16], [20], and these NNLS problems can be solved by the well-known active set based algorithm [19].

Table I compares the complexity (including computing the closed forms (17) and (19)) between CI-WMMSE and the optimal NNLS-based solution of CI-ZF in [20], which requires minimum complexity among several optimal solution forms of CI-ZF [6], [7], [20]. We omit the derivation of complexity because it only involves simple calculations. '(LC)' indicates that the NNLS problem is simplified by our low-complexity algorithmic solution. $N_{L1}/N_{L2}/N_{L3}$ denote the numbers of main loops in active set based algorithm. $\mathbb{E}\{M\}$ denotes the average M with Rayleigh channel in SNR range from 0 to 40dB. N_M is the number of multiplications that should be performed when a matrix with dimension $2N \times 2K$ multiplies a matrix with dimension $2K \times 2K$. As Table I shows, our design in this subsection reduces part of the complexity, and CI-WMMSE has a similar low complexity to CI-ZF.

TABLE I
COMPLEXITY (REQUIRED MULTIPLICATIONS) COMPARISON

	Required Multiplication Number M	$\mathbb{E}\{M\}$ ($N = K = 12$)
CI-WMMSE (LC)	$(8N + 4K_\tau + 4K_\tau N_{L1})K$ $+(12 + 16N + 13\frac{1}{3}K)K^2$	$4.09N_M$ $3.94N_M$
CI-ZF [20]	$(20K + 8KN_{L2})N$ $+(4 + 24N + 4K)K^2$	$4.17N_M$ $3.92N_M$
CI-ZF (LC)	$(4K_\tau + 12K + 4K_\tau N_{L3})N$ $+(4 + 24N + 4K)K^2$	$3.99N_M$ $3.76N_M$

IV. NUMERICAL RESULTS

In this section, we use the Monte Carlo method to evaluate the performance in the scenario of the Rayleigh fading channel. Since the designs of \mathbf{A} and Ω are beyond the scope of the present work, we consider the special case of $\mathbf{A} = \mathbf{I}$ and $\Omega = \mathbf{I}$ during the simulation to highlight our contribution, based on which CI-WMMSE degenerates into CI-MMSE. It is assumed that a transmission block consists of L groups of symbols, within whose time-frequency resource the wireless channel stays fixed. To facilitate the practical demodulation for the SLP schemes involved in the simulation, we unify the γ in each transmission block by employing the power allocation scheme in [8].

Fig. 3 shows the comparison of SER performance for $N = K = 12$, in which the performance comparison in the low SNR ranges is magnified and displayed in the lower left. In order to be consistent with the most conventional SLP studies [6], [10], [14], we consider $L = 1$ in Fig. 3. It can be observed that

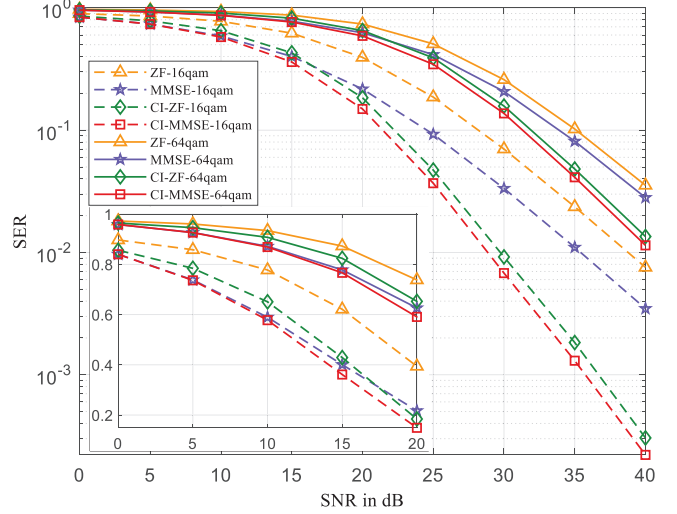


Fig. 3. SER vs SNR, $N = K = 12$, symbol transmission ($L = 1$).

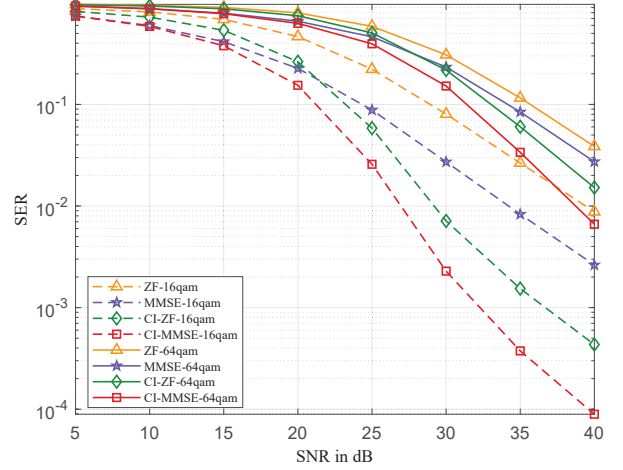


Fig. 4. SER vs SNR, $N = K = 12$, block transmission ($L = 1000$).

CI-MMSE achieves a significant gain than MMSE, and it also provides better performance than CI-ZF in full SNR ranges. The SER comparison with $L = 1000$ is shown in Fig. 4. CI-MMSE provides SNR gains of about 2.3dB and 7.4dB than CI-ZF and MMSE when the SER is 10^{-2} with 16QAM, and a similar trend can also be observed in 64QAM transmission. There exist some performance differences between Fig. 3 and Fig. 4 since small L has an impact on the SLP performance with power allocation [8].

Fig. 5 compares the spectrum efficiency of the different techniques with the low-density parity check (LDPC) coding scheme [22]. Since the received signals of the external constellation are extended and do not follow Gaussian distribution, the variance provided for the Gaussian soft demodulator is computed from the received signals of the inner constellation. We simulate the adaptive coding, which has not been studied in SLP, by decreasing the code rate from high to low to find the best-matched one for data transmission. Compared with CI-ZF, CI-MMSE provides about 37.8% gain in spectrum efficiency

when SNR is 15dB with 16QAM and 38.9% gain when SNR is 20dB with 64QAM. It is worth noting that CI-MMSE provides better performance in full SNR ranges in both coded and uncoded systems.

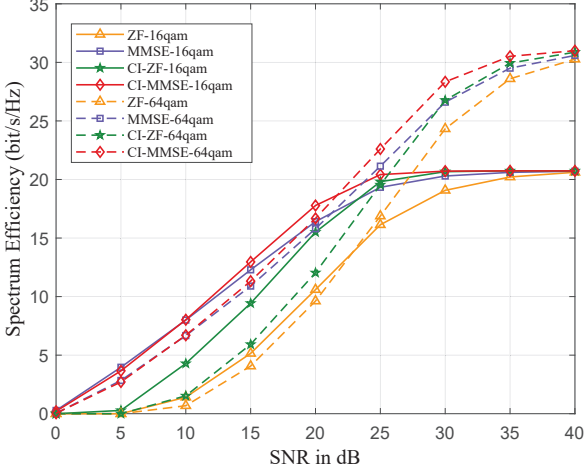


Fig. 5. Spectrum Efficiency vs SNR, $N = K = 12$, LDPC, $L = 6000$.

V. CONCLUSION

In this paper, we propose the CI-WMMSE symbol-level precoding, which minimizes the weighted mean square error between the received signal and the constellation point in CIR. In addition, we first put forward a simple generic description of CIR that facilitates subsequent SLP design. Based on the latter, the CI-WMMSE is further formulated as an NNLS problem that can be solved efficiently by the active-set algorithm. Besides, the WMMSE precoding and the existing SLP solutions can be easily verified as special cases of the proposed scheme. The simulation results show that CI-WMMSE outperforms the state-of-the-art SLP schemes in full SNR ranges in both coded and uncoded systems without additional complexity over conventional SLP.

REFERENCES

- [1] A. Bourdoux and N. Khaled, "Joint TX-RX optimisation for MIMO-SDMA based on a null-space constraint," in *Proc. IEEE 56th Veh. Technol. Conf. (VTC)*, vol. 1, Sept. 2002, pp. 171–174.
- [2] H. Sampath, P. Stoica, and A. Paulraj, "Generalized linear precoder and decoder design for mimo channels using the weighted MMSE criterion," *IEEE Trans. Commun.*, vol. 49, no. 12, pp. 2198–2206, Dec. 2001.
- [3] M. Costa, "Writing on dirty paper (corresp.)," *IEEE Trans. Inf. Theory*, vol. 29, no. 3, pp. 439–441, May 1983.
- [4] B. Hochwald, C. Peel, and A. Swindlehurst, "A vector-perturbation technique for near-capacity multiantenna multiuser communication-part II: Perturbation," *IEEE Trans. Commun.*, vol. 53, no. 3, pp. 537–544, Jan. 2005.
- [5] A. Li, D. Spano, J. Krivochiza, S. Domouchtsidis, C. G. Tsinos, C. Masouros, S. Chatzinotas, Y. Li, B. Vucetic, and B. Ottersten, "A tutorial on interference exploitation via symbol-level precoding: Overview, state-of-the-art and future directions," *IEEE Commun. Surveys Tuts.*, vol. 22, no. 2, pp. 796–839, Mar. 2020.
- [6] A. Li, C. Masouros, B. Vucetic, Y. Li, and A. L. Swindlehurst, "Interference exploitation precoding for multi-level modulations: Closed-form solutions," *IEEE Trans. Commun.*, vol. 69, no. 1, pp. 291–308, Jan. 2021.
- [7] C. Masouros and G. Zheng, "Exploiting known interference as green signal power for downlink beamforming optimization," *IEEE Trans. Signal Process.*, vol. 63, no. 14, pp. 3628–3640, Jul. 2015.
- [8] A. Li, F. Liu, X. Liao, Y. Shen, and C. Masouros, "Symbol-level precoding made practical for multi-level modulations via block-level rescaling," in *IEEE Workshop Signal Process. Adv. Wireless Commun. (SPAWC)*, Lucca, Italy, Sept. 2021, pp. 71–75.
- [9] M. Alodeh, S. Chatzinotas, and B. Ottersten, "Constructive interference through symbol level precoding for multi-level modulation," in *IEEE Glob. Commun. Conf. (GLOBECOM)*, San Diego, CA, USA, Dec. 2015, pp. 1–6.
- [10] A. Li and C. Masouros, "Interference exploitation precoding made practical: Optimal closed-form solutions for PSK modulations," *IEEE Trans. Wireless Commun.*, vol. 17, no. 11, pp. 7661–7676, Sept. 2018.
- [11] A. Haqiqatnejad, F. Kayhan, and B. Ottersten, "Constructive interference for generic constellations," *IEEE Signal Process. Lett.*, vol. 25, no. 4, pp. 586–590, Apr. 2018.
- [12] A. Haqiqatnejad, F. Kayhan, and B. Ottersten, "Symbol-level precoding design based on distance preserving constructive interference regions," *IEEE Trans. Signal Process.*, vol. 66, no. 22, pp. 5817–5832, Nov. 2018.
- [13] C. Masouros and E. Alsusa, "Dynamic linear precoding for the exploitation of known interference in MIMO broadcast systems," *IEEE Trans. Wireless Commun.*, vol. 8, no. 3, pp. 1396–1404, Mar. 2009.
- [14] M. Alodeh, S. Chatzinotas, and B. Ottersten, "Constructive multiuser interference in symbol level precoding for the MISO downlink channel," *IEEE Trans. Signal Process.*, vol. 63, no. 9, pp. 2239–2252, May 2015.
- [15] Y. Liu and W.-K. Ma, "Symbol-level precoding is symbol-perturbed zf when energy efficiency is sought," in *IEEE Int. Conf. Acoust., Speech Signal Process. (ICASSP)*, Calgary, AB, Canada, Apr. 2018, pp. 3869–3873.
- [16] J. Krivochiza, A. Kalantari, S. Chatzinotas, and B. Ottersten, "Low complexity symbol-level design for linear precoding systems," *Proc. Symp. Inf. Theory Signal Process. Benelux*, pp. 1–8, 2017.
- [17] S. S. Christensen, R. Agarwal, E. De Carvalho, and J. M. Cioffi, "Weighted sum-rate maximization using weighted MMSE for MIMO-BC beamforming design," *IEEE Trans. Wireless Commun.*, vol. 7, no. 12, pp. 4792–4799, Dec. 2008.
- [18] C. Peel, B. Hochwald, and A. Swindlehurst, "A vector-perturbation technique for near-capacity multiantenna multiuser communication-part I: Channel inversion and regularization," *IEEE Trans. Commun.*, vol. 53, no. 1, pp. 195–202, Jan. 2005.
- [19] C. L. Lawson and R. J. Hanson, *Solving least squares problems*. SIAM, 1995.
- [20] A. Haqiqatnejad, F. Kayhan, and B. Ottersten, "An approximate solution for symbol-level multiuser precoding using support recovery," in *IEEE Workshop Signal Process. Adv. Wireless Commun. (SPAWC)*, Cannes, France, Jul. 2019, pp. 1–5.
- [21] M. Joham, K. Kusume, M. Gzara, W. Utschick, and J. Nossek, "Transmit wiener filter for the downlink of TD-DS-CDMA systems," in *Proc. IEEE 7th Symp. Spread-Spectrum Technol.*, vol. 1, Applicat., Prague, Czech Republic, Sep. 2002, pp. 9–13.
- [22] R. Gallager, "Low-density parity-check codes," *IRE Trans. Inf. Theory*, vol. 8, no. 1, pp. 21–28, Jan. 1962.